This is a preprint, the final version is subject to change, of the American Mineralogist (MSA)
Cite as Authors (Year) Title. American Mineralogist, in press.
DOI: https://doi.org/10.2138/am-2018-6464

Temperature and pressure effects on the partitioning of V and Sc between clinopyroxene and silicate melt: Implications for mantle oxygen fugacity

YUAN LI[1,2*]

[1]State Key Laboratory of Isotope Geochemistry, Guangzhou Institute of Geochemistry, Chinese Academy of Sciences, Guangzhou 510640, China

[2]Bayerisches Geoinstitut, University Bayreuth, 95440 Bayreuth, Germany

ABSTRACT

The partition coefficients of V and Sc between clinopyroxene and silicate melt ($D_V^{Cpx/SM}$ *and* $D_{Sc}^{Cpx/SM}$) have been determined experimentally at 1200-1400 °C and 0.8-2.3 GPa, using a hornblende- and clinopyroxene-rich mantle rock in graphite-lined $Pt_{95}Rh_{05}$ capsules. The results show that the $D_V^{Cpx/SM}$ and $D_{Sc}^{Cpx/SM}$ values decrease from 3.8 to 2.3 and from 2.6 to 1.1, respectively, as the experimental temperature and pressure vary from 1200 °C and 0.8 GPa to 1400 °C and 2.3 GPa. The presence of water in silicate melts may also reduce $D_V^{Cpx/SM}$ and $D_{Sc}^{Cpx/SM}$. These results imply that the effects of temperature, pressure, and melt water content on $D_V^{Cpx/SM}$ should be considered when using V systematics in cratonic mantle peridotites to constrain cratonic mantle oxygen fugacity (fO_2). However, although the dominant V in the present silicate melt is mixed

* Email address: Yuan.Li@gig.ac.cn

This is a preprint, the final version is subject to change, of the American Mineralogist (MSA)
Cite as Authors (Year) Title. American Mineralogist, in press.
DOI: https://doi.org/10.2138/am-2018-6464

V^{3+} and V^{4+}, the $D_V^{Cpx/SM}/D_{Sc}^{Cpx/SM}$ together with literature data obtained at similar fO_2 shows a nearly constant value of 1.68±0.26, regardless of temperature, pressure, melt composition, and melt water content, indicating that these factors cannot cause fractionation of Sc^{3+} from mixed V^{3+} and V^{4+} in mantle melts through clinopyroxene/silicate melt partitioning. Therefore, in combination with V/Sc systematics in primitive MORBs and arc basalts, using $D_V^{Cpx/SM}$ and $D_{Sc}^{Cpx/SM}$ obtained at 1 bar and dry conditions should be valid to constrain mantle fO_2, except for the case that the $D^{Cpx/SM}$ for Sc^{3+} can be demonstrated to be fractionated from the $D^{Cpx/SM}$ for mixed V^{4+} and V^{5+} which are present in oxidized basalts.

Keywords: oxygen fugacity, upper mantle, Vanadium, Scandium, partitioning, clinopyroxene, silicate melt

INTRODUCTION

Oxygen fugacity (fO_2) is an important parameter that can significantly affect the geochemical and geophysical properties of Earth's mantle material. The fO_2 of MORBs is mainly between FMQ-1 and FMQ, and the fO_2 of arc basalts is higher than that of MORBs, as evidenced by the higher $Fe^{3+}/\sum Fe$ in arc basalts (e.g., Frost and McCammon 2008; Kelley and Cottrell 2009, 2012; Brounce et al. 2014, 2015). However, whether the oxidized nature of arc basalts is inherited from the subarc mantle or is derived from magmatic differentiation processes occurring in the crust remains debated (e.g., Evans et al. 2012; Grocke et al. 2016; Lee et al. 2005, 2010; Brounce et al. 2015). The clear

This is a preprint, the final version is subject to change, of the American Mineralogist (MSA)
Cite as Authors (Year) Title. American Mineralogist, in press.
DOI: https://doi.org/10.2138/am-2018-6464

correlation between $Fe^{3+}/\sum Fe$ and water content in undegassed, olivine-hosted basaltic melt inclusions was used to argue for a high fO_2 in the subarc mantle, which could be caused by fluid fluxing of the subducted slab (Kelley and Cottrell 2012; Brounce et al. 2014, 2015). This argument is supported by measurements of spinel compositions in primitive arc lavas, which imply the subarc mantle 1-4 log units more oxidized than the oceanic mantle (Evans et al. 2012). Nevertheless, based on the partitioning of V and Sc between mantle minerals and silicate melts ($D^{Mineral/SM}$) and the similarity of V/Sc in primitive MORBs and arc basalts, Lee et al. (2005) and Mallmann and O'Neill (2009) concluded that the fO_2 of the subarc mantle and the oceanic mantle is similar. However, the $D_V^{Mineral/SM}$ and $D_{Sc}^{Mineral/SM}$ data used in these two studies were calibrated for one atmosphere pressure (1 bar) and dry conditions (Canil 1997, 1999; Canil and Fedortchouk 2000; Mallmann and O'Neill 2009), and fO_2 was assumed to be the only factor causing fractionation of $D_V^{Mineral/SM}$ from $D_{Sc}^{Mineral/SM}$ and thus the variation of V/Sc in primitive basalts. The effects of pressure and temperature (*P*-*T*) on $D_V^{Mineral/SM}$ and $D_{Sc}^{Mineral/SM}$ remain indeed uninvestigated, but which could be important to constrain mantle fO_2. For example, if *P*-*T* cause fractionation of $D_V^{Mineral/SM}$ from $D_{Sc}^{Mineral/SM}$ at a given fO_2, and if the melting *P*-*T* for the genesis of MORBs and arc basalts are not always the same, opposed to what assumed in Lee et al. (2005) and Mallmann and O'Neill (2009), then the similar V/Sc in primitive MORBs and arc basalts does not necessarily imply a similar fO_2 of the subarc mantle and the oceanic mantle. Therefore, to ensure that the variation of V/Sc in primitive MORBs and arc basalts are only caused by the heterogeneity in mantle fO_2, and the similar V/Sc reflects a similar fO_2

This is a preprint, the final version is subject to change, of the American Mineralogist (MSA)
Cite as Authors (Year) Title. American Mineralogist, in press.
DOI: https://doi.org/10.2138/am-2018-6464

of the subarc mantle and the oceanic mantle, the *P*-*T* effects on $D_V^{Mineral/SM}$ and $D_{Sc}^{Mineral/SM}$ should be determined simultaneously.

In the Earth's upper mantle V and Sc are mainly stored in clinopyroxene, and the $D_V^{Cpx/SM}$ and $D_{Sc}^{Cpx/SM}$ as a function of fO_2 have been well calibrated at 1bar (Canil and Fedortchouk 2000; Mallmann and O'Neill 2009). I here therefore determine the effects of *P*-*T* on $D_V^{Cpx/SM}$ and $D_{Sc}^{Cpx/SM}$, so as to see if variation of the mantle melting *P*-*T* can cause fractionation of V from Sc in primitive MORBs and arc basalts. Determining the *P*-*T* effects on $D_V^{Cpx/SM}$ would also have important implications for the cratonic mantle fO_2 constrained previously using V systematics alone and $D_V^{Cpx/SM}$ obtained at 1 bar (Canil 2002; Lee et al. 2003).

EXPERIMENTAL AND ANALYTICAL MTHODS

The starting material is a natural mantle rock, which stems from a hornblende- and clinopyroxene-rich, metasomatic vein in orogenic peridotite of the French Pyrenees and has a chemical composition of 43.31 wt.% SiO_2, 11.23 wt.% Al_2O_3, 17.07 wt.% CaO, 12.53 wt.% MgO, 7.65 wt.% FeO, 3.59 wt.% TiO_2, 1.60 wt.% Na_2O, 0.81 wt.% K_2O, 0.05 wt.% P_2O_5, 0.12 wt.% MnO, 0.76 wt.% H_2O, and 0.26 wt.% CO_2 (Fabries et al. 2001; Pilet et al. 2008). The same starting silicate was used in the experiments of Pilet et al. (2008) to study the origin of alkaline magmas, and the adoption of this silicate here is to attempt to grow relatively big clinopyroxene crystals. In all experiments the starting silicate was placed into a graphite capsule (4.5 mm O.D.; 3.6 mm I.D.; 7 mm length),

This is a preprint, the final version is subject to change, of the American Mineralogist (MSA)
Cite as Authors (Year) Title. American Mineralogist, in press.
DOI: https://doi.org/10.2138/am-2018-6464

which was then loaded into a $Pt_{95}Rh_{05}$ capsule (5.0 mm O.D.; 4.6 mm I.D.; 10 mm length). All the experiments were conducted at 1200-1400 °C and 0.5-2.3 GPa in an end-loaded, solid media piston cylinder apparatus, using 0.5/0.75-inch diameter Talc-Pyrex assemblies with tapered graphite heaters. In order to grow clinopyroxene crystals, the experimental *P*-*T* were covaried (Table 1). The hot piston-in method was used to pressurize the assembly, and a friction correction of ~18% was applied based on calibration of the quartz-coesite and kyanite-sillimanite transitions. The pressure uncertainty is about 0.1 GPa. The temperature was monitored by Pt-$Pt_{90}Rh_{10}$ (S-type) thermocouples with an uncertainty of ~10 °C. All the experiments were run for 24 hours, except for run Y-4 for 48 hours (Table 1), and were quenched by switching off the electricity to the graphite heaters.

The major element compositions of quenched silicate melts and minerals were measured with a JEOL JXA-8200 microprobe. The analyses were performed in wavelength-dispersive mode, and a PAP matrix correction was applied to the raw data. The quenched silicate melts and minerals were analyzed with 15 kV / 10 nA, with defocused beams of 30 and 10 μm diameter used, respectively, for all the standardizations and sample measurements. Both natural and synthetic standards were used to calibrate the instrument, as described in Li and Audétat (2015).

Trace element analyses of V, Sc, Zr and Hf in silicate melts and minerals were carried out on an Agilent 7900 Quadrupole ICP-MS coupled to a Photon Machines Analyte HE 193-nm ArF Excimer Laser Ablation system. A squid signal smoothing device is included in this laser ablation system. Helium was applied as the carrier gas, and nitrogen gas was used as the makeup gas and mixed with the carrier gas via a T-

This is a preprint, the final version is subject to change, of the American Mineralogist (MSA)
Cite as Authors (Year) Title. American Mineralogist, in press.
DOI: https://doi.org/10.2138/am-2018-6464

connector before entering the ICP. After measuring the gas blank for 20s, each analysis was performed by a laser beam of 30-50 μm diameter for silicate minerals, and of 50 μm diameter for silicate melts, at 8 Hz with energy of ~2 J/cm^2 for 40s. NIST SRM 610 glass was used as external standard for all analyses, whereas Si determined by electron microprobe was used as internal standard. Overall analytical uncertainties arising from the internal and external standardization procedure are better than 10% for trace elements.

RESULTS AND DISCUSSION

Experimental conditions and run products are summarized in Table 1. Representative run products are shown in Figure 1. Clinopyroxene crystals are present in all runs, with a few olivine crystals present in the runs at pressures below 1.4 GPa. The volume fraction of silicate melts in the sample capsules ranges between 40% and 90%, increasing with increasing temperature and decreasing pressure. The measured major and trace element compositions of clinopyroxene crystals and silicate melts are given in Table 1. Clinopyroxene crystals contain about 0.21-0.61 wt.% Na_2O, 13.83-16.98 wt.% MgO, 6.44-8.53 wt.% Al_2O_3, 48.25-50.65 wt.% SiO_2, 22.69-24.24 wt.% CaO, 2.14-4.27 wt.% FeO, and 1.04-2.34 wt.% TiO_2. The V, Sc, Zr, and Hf contents in clinopyroxene are about 704-1014 ppm, 74-124 ppm, 10-69 ppm, and 0.8-2.9 ppm, respectively. The silicate melts contain 1.4-2.7 wt.% Na_2O, 8.42-11.87 wt.% MgO, 11.9-14.18 wt.% Al_2O_3, 39.66-42.52 wt.% SiO_2, 0.9-1.21 wt.% K_2O, 15.2-17.18 wt.% CaO, 5.16-8.74 wt.% FeO, and 3.98-4.51 wt.% TiO_2. The melt water content should be about 1-2 wt.%, according to

This is a preprint, the final version is subject to change, of the American Mineralogist (MSA)
Cite as Authors (Year) Title. American Mineralogist, in press.
DOI: https://doi.org/10.2138/am-2018-6464

the degree of melting and the water content in the starting silicate. Consistent with Pilet et al. (2008), the silicate melts are typical basanitic melts. The V, Sc, Zr, and Hf contents in silicate melts are about 192-327 ppm, 39-66 ppm, 120-147 ppm, and 3.5-4.5 ppm, respectively.

The calculated $D^{Cpx/SM}$ values for V, Sc, Zr, and Hf are summarized in Table 1 and illustrated in Figure 2. The nearly identical $D^{Cpx/SM}$ for V and Sc in runs Y-1 and Y-4 with run duration of 24 and 48 hours, respectively, and the clear temperature dependence of $D^{Cpx/SM}$ (see below) imply that 24 hours is sufficient to achieve equilibrium partitioning. All $D^{Cpx/SM}$ values, 2.3-3.8 for V, 1.1-2.6 for Sc, 0.08-0.58 for Zr, and 0.18-0.71 for Hf, decrease with increasing temperature (Fig. 2; Table 1), although the pressure varies from 0.8 to 2.3 GPa. This indicates that increasing pressure may also result in a decrease in $D^{Cpx/SM}$, or that pressure does not considerably affect $D^{Cpx/SM}$. Moreover, the slopes of regression of the $D^{Cpx/SM}$ data for V and Sc are very close to each other (Fig. 2a), as in the case for Zr and Hf (not shown), which suggests that V and Sc share very similar partitioning behavior between clinopyroxene and silicate melt, and hence that *P-T* do not cause fractionation of V from Sc in mantle melts through clinopyroxene/silicate melt partitioning. Previous experimental studies show that the $D^{Cpx/SM}$ values for Sc, Zr, and Hf all decrease with increasing temperature and/or pressure (Bédard 2014; Hill et al. 2010); thus the $D_V^{Cpx/SM}$ should also decrease with increasing pressure.

The $D_V^{Cpx/SM}/D_{Sc}^{Cpx/SM}$ and $D_{Zr}^{Cpx/SM}/D_{Hf}^{Cpx/SM}$, together with literature data, are plotted as a function of temperature in Figure 3. It can be seen from Figure 3 that the

This is a preprint, the final version is subject to change, of the American Mineralogist (MSA)
Cite as Authors (Year) Title. American Mineralogist, in press.
DOI: https://doi.org/10.2138/am-2018-6464

152 $D_{Zr}^{Cpx/SM}/D_{Hf}^{Cpx/SM}$ is nearly a constant of 0.52 ± 0.10, which is consistent with the
153 consensus that Zr and Hf are rarely fractionated from each other during mantle melting.
154 The $D_{V}^{Cpx/SM}/D_{Sc}^{Cpx/SM}$ is between 1.4 and 2, and is also a constant within error ($1.68 \pm$
155 0.26), except for one literature value up to 3 but with a large uncertainty. It should be
156 noted that the $D^{Cpx/SM}$ values for V, Sc, Zr, and Hf plotted in Figure 3 were obtained at a
157 large range of *P-T* conditions (0.8-3.5 GPa and 1050-1470 °C). Accordingly, the nearly
158 constant $D_{V}^{Cpx/SM}/D_{Sc}^{Cpx/SM}$ (1.68 ± 0.26) again suggests that *P-T* may not cause
159 fractionation of V from Sc in mantle melts through clinopyroxene/silicate melt
160 partitioning.

161 The $D^{Cpx/SM}$ for trace elements is a multiple function of not only *P-T* but also crystal
162 chemistry, melt composition, melt water content, and fO_2 (Bédard 2014; Canil 1997; Hill
163 et al. 2010; Lundstrom et al. 1998; Mallmann and O'Neill 2013; Michely et al. 2017;
164 Wood and Blundy 2002). Sc is an element with a valence state of 3+ at the Earth's upper
165 mantle conditions, and $D_{Sc}^{Cpx/SM}$ is thus insensitive to the variation of mantle fO_2
166 (Mallmann and O'Neill 2009). However, V can be present as V^{2+}, V^{3+}, V^{4+}, and V^{5+} in the
167 Earth's upper mantle, and $D_{V}^{Cpx/SM}$ is thus very sensitive to the variation of mantle fO_2
168 (Canil and Fedortchouk 2000; Mallmann and O'Neill 2009). In this study, the fO_2 was not
169 controlled but should be around the C-CO_2 buffer because of the used graphite-lined
170 $Pt_{95}Rh_{05}$ capsule. Many studies show that the fO_2 prevailing in the experiments performed
171 in graphite-lined Pt or $Pt_{95}Rh_{05}$ capsules is ~FMQ-2 (Canil and Fedortchouk 2000; Li and
172 Audétat 2012, 2015; Médard et al. 2008). For example, the fO_2 of an experiment

This is a preprint, the final version is subject to change, of the American Mineralogist (MSA)
Cite as Authors (Year) Title. American Mineralogist, in press.
DOI: https://doi.org/10.2138/am-2018-6464

performed at 1200 °C and 1.5 GPa in a graphite-lined $Pt_{95}Rh_{05}$ capsule to study element partitioning between sulfide phases and basanitic melt was determined to be FMQ-2.1 based on Mössbauer-Spectrometry measured $Fe^{3+}/\sum Fe$ in the basanitic melt (Li and Audétat 2012). At fO_2 of ~FMQ-2, V could be present mainly as mixed V^{3+} and V^{4+} in the silicate melt (Sutton et al. 2005; Righter et al. 2006). For example, the valence state of V in a Hawaiian ankaramitic basalt at 1300 °C and fO_2 of ~FMQ-2 is ~3.5, determined by vanadium K-edge X-ray absorption near edge structure (XANES) spectroscopy (Righter et al. 2006). Therefore, the present study indeed demonstrates that *P-T* cannot fractionate mixed V^{3+} and V^{4+} from Sc^{3+} in mantle melts through clinopyroxene/silicate melt partitioning. The presence of a considerable amount of water in silicate melt may reduce the $D^{Cpx/SM}$ for trace elements (Wood and Blundy 2002), which may partly explain the relatively low $D_V^{Cpx/SM}$ and $D_{Sc}^{Cpx/SM}$ values obtained in Adam and Green (2006) (Fig. 2b), in which study 6-16 wt.% water was present in the silicate melts. The effect of melt composition on $D^{Cpx/SM}$ cannot be readily assessed in this study, because available experiments were performed not only using different starting silicates but also at different *P-T* conditions (Fig. 2b). However, the location of the $D_V^{Cpx/SM}$ and $D_{Sc}^{Cpx/SM}$ data points obtained in Davis et al. (2013) on the data trend obtained in this study indicates that the effect of melt composition difference in these two studies on $D^{Cpx/SM}$ may just be negligible compared to that of temperature (see Fig. 2b). More importantly, the nearly constant $D_V^{Cpx/SM}/D_{Sc}^{Cpx/SM}$ (Fig. 3) implies that neither the variation of melt composition nor the presence of a significant amount of water in silicate melt can fractionate the $D^{Cpx/SM}$ for mixed V^{3+} and V^{4+} from the $D^{Cpx/SM}$ for Sc^{3+}.

The present study demonstrates that the variation of *P-T*, melt composition, and melt water content cannot cause fractionation of the $D^{Cpx/SM}$ for mixed V^{3+} and V^{4+} from the $D^{Cpx/SM}$ for Sc^{3+}. However, according to the calibrated V valence state as a function of fO_2 in basaltic melts (Sutton et al. 2005; Righter et al. 2006), mixed V^{4+} and V^{5+} can also be present in the Earth's natural basalts if the fO_2 is above FMQ. Therefore, whether the $D^{Cpx/SM}$ for mixed V^{4+}+V^{5+} can be fractionated from the $D^{Cpx/SM}$ for Sc^{3+} due to variation of the above-mentioned factors remains to be constrained.

IMPLICATIONS FOR MANTLE OXYGEN FUGACITY

The present study shows that the $D^{Cpx/SM}$ for both V and Sc is a function of temperature, pressure, and probably melt water content. Therefore, to constrain mantle fO_2 using V systematics in mantle peridotites, the effects of temperature, pressure, and melt water content on $D_V^{Cpx/SM}$ should be considered. Canil (2002) and Lee et al. (2003) used the $D_V^{Cpx/SM}$ data obtained at 1 bar and dry conditions to constrain the cratonic mantle fO_2 by modelling V contents in cratonic mantle peridotites. This study thus implies that the error for the cratonic mantle fO_2 constrained in these previous studies can be significant. The error for the cratonic mantle fO_2 constrained previously, introduced by using $D_V^{Cpx/SM}$ data obtained at 1 bar and dry conditions, can be illustrated below by performing a simple calculation of V contents in cratonic mantle peridotites. Firstly, I assume partial melting of mantle peridotite occurs at 1700 °C and 7 GPa and at fO_2 of FMQ-2, which corresponds to ~20% melting and which is highly possible for the genesis of some cratonic mantle peridotites (Walter 1998; Canil 2002). Secondly, I use $D_V^{Cpx/SM}$

This is a preprint, the final version is subject to change, of the American Mineralogist (MSA)
Cite as Authors (Year) Title. American Mineralogist, in press.
DOI: https://doi.org/10.2138/am-2018-6464

of 1.5 and $D_V^{Olivine/SM}$ of 0.09 obtained at ~1300 °C and 1 bar (Canil 1997, Canil and Fedortchouk 2000) and $D_V^{Garnet/SM}$ of 1 (Canil 2002), as have been used in Canil (2002) and Lee et al. (2003) at fO_2 of FMQ-2. Using the calculation method in Lee et al. (2003), the calculated V content in the cratonic mantle peridotite after melt extraction is ~64 ppm. Simply, if we now only consider the *P*-*T* effect on $D_V^{Cpx/SM}$ and assume that the *P*-*T* variation from 1300 °C and 1 bar to 1700 °C and 7 GPa only decreases $D_V^{Cpx/SM}$ by a factor of 2, then the calculated V content in the cratonic mantle peridotite is ~42 ppm. This value can only be achieved at ~FMQ-0.5 if the *P*-*T* effect on $D_V^{Cpx/SM}$ is not taken into account (Lee et al. 2003). Note that the variation of *P*-*T* from 1200 °C and 0.8 GPa to 1400 °C and 2.3 GPa in this study already decreases $D_V^{Cpx/SM}$ by factor of 1.65. Therefore, these calculations demonstrate that significant error can be introduced for the estimated cratonic mantle fO_2 if the $D_V^{Cpx/SM}$ obtained at 1300 °C and 1 bar is used and if the *P*-*T* effect on $D_V^{Cpx/SM}$ is ignored. Also, the previously estimated fO_2 for the cratonic mantles generated by high *P*-*T* melt extraction (Canil 2002; Lee et al. 2003), such as the Siberian cratonic mantle, should be considerably higher than the actual fO_2.

The present study also shows that the $D_V^{Cpx/SM}/D_{Sc}^{Cpx/SM}$ does not vary as the variation of *P*-*T*, melt composition, and melt water content; in this case only the variation of fO_2 can cause fractionation of $D_V^{Cpx/SM}$ from $D_{Sc}^{Cpx/SM}$. Therefore, V/Sc should be more robust than V alone in recording fO_2 of the mantle source regions of basalts. Consequently, the use of $D_V^{Cpx/SM}$ and $D_{Sc}^{Cpx/SM}$ obtained at 1 bar and dry conditions and the use of V/Sc in the Archean basalts and MORBs (Li and Lee 2004) should be valid to

This is a preprint, the final version is subject to change, of the American Mineralogist (MSA)
Cite as Authors (Year) Title. American Mineralogist, in press.
DOI: https://doi.org/10.2138/am-2018-6464

constrain their mantle fO_2 (Fig. 3), considering that V in these basalts should be present mainly as mixed V^{3+} and V^{4+} (Sutton et al. 2005). The invariance of $D_V^{Cpx/SM}/D_{Sc}^{Cpx/SM}$ also supports, at least in part, the studies of Lee et al. (2005) and Mallmann and O'Neill (2009), in which the similar V/Sc in primitive MORBs and arc basalts was used to argue for a similar fO_2 in their mantle source regions, by assuming fO_2 being the only factor causing fractionation of $D_V^{Cpx/SM}$ from $D_{Sc}^{Cpx/SM}$. The reason for not fully supporting the studies of Lee et al. (2005) and Mallmann and O'Neill is due to the fact that the present study does not demonstrate non-fractionation of the $D^{Cpx/SM}$ for Sc^{3+} from the $D^{Cpx/SM}$ for mixed V^{4+} and V^{5+} which are present in oxidized basalts with $fO_2 >$ FMQ. Whether *P*-*T*, melt composition, and melt water content can cause fractionation of the $D^{Cpx/SM}$ for Sc^{3+} from the $D^{Cpx/SM}$ for mixed V^{4+} and V^{5+} actually needs further investigation. In order to fully understand the link between mantle fO_2 and V/Sc systematics in primitive basalts, the $D^{Mineral/SM}$ for both V and Sc as a function of *P*-*T*, melt composition, and melt water content should also be determined at largely variable fO_2s in the future. In addition, the difference of the sub-arc mantle and the oceanic mantle in modal composition or peridotite fertility should also be considered when using V/Sc systematics to constrain mantle fO_2, this is because different peridotite fertilities must result in different bulk partition coefficients for both V and Sc even if mantle partial melting takes place at the same fO_2.

ACKNOWLEGEMENTS

Support from the Recruitment Program of Global Young Experts (PR China) is appreciated. Constructive reviews by Maryjo Brounce, Ian Swainson, and two anonymous reviewers significantly improved this paper.

This is a preprint, the final version is subject to change, of the American Mineralogist (MSA)
Cite as Authors (Year) Title. American Mineralogist, in press.
DOI: https://doi.org/10.2138/am-2018-6464

263 **REFERENCES CITED**

264 Adam, J., and Green, T. (2006) Trace element partitioning between mica-and amphibole-
265 bearing garnet lherzolite and hydrous basanitic melt: 1. Experimental results and the
266 investigation of controls on partitioning behaviour. Contributions to Mineralogy and
267 Petrology, 152, 1-17.

268 Bédard, J.H. (2014) Parameterizations of calcic clinopyroxene-Melt trace element
269 partition coefficients. Geochemistry, Geophysics, Geosystems, 15, 303-336.

270 Brounce, M., Kelley, K. A., Cottrell, E. (2014) Variations in $Fe^{3+}/\sum Fe$ of Mariana Arc
271 Basalts and Mantle Wedge fO2. Jounral of Petrology, 55, 2513-2536.

272 Brounce, M., Kelley, K. A., Cottrell, E., and Reagan, M. K. (2015) Temporal evolution
273 of mantle wedge oxygen fugacity during subduction initiation. Geology, 43, 775-778.

274 Canil, D. (1997) Vanadium partitioning and the oxidation state of Archaean komatiite
275 magmas. Nature 389, 842-845.

276 Canil, D. (1999) Vanadium partitioning between orthopyroxene, spinel and silicate melt
277 and the redox states of mantle source regions for primary magmas. Geochimica et
278 Cosmochimica Acta, 63, 557-572.

279 Canil, D. (2002) Vanadium in peridotites, mantle redox and tectonic environments:
280 Archean to present. Earth and Planetary Science Letters, 195, 75-90.

281 Canil, D., and Fedortchouk, Y. (2000) Clinopyroxene-liquid partitioning for vanadium
282 and the oxygen fugacity during formation of cratonic and oceanic mantle lithosphere.
283 Journal of Geophysical Research: Solid Earth, 105, 26003-26016.

284 Davis, F. A., Humayun, M., Hirschmann, M. M., and Cooper, R. S. (2013)
285 Experimentally determined mineral/melt partitioning of first-row transition elements
286 (FRTE) during partial melting of peridotite at 3GPa. Geochimica et Cosmochimica
287 Acta, 104, 232-260.

288 Evans, K.A., Elburg, M.A., and Kamenetsky, V.S. (2012) Oxidation state of subarc
289 mantle. Geology 40, 783-786.

290 Fabries, J., Lorand, J.-P., and Guiraud, M. (2001) Petrogenesis of the amphibole-rich
291 veins from the Lherz orogenic lherzolite massif (Eastern Pyrenees, France): a case
292 study for the origin of orthopyroxene-bearing amphibole pyroxenites in the
293 lithospheric mantle. Contributions to Mineralogy and Petrology, 140, 383-403.

294 Frost, D.J., and McCammon, C.A. (2008) The Redox State of Earth's Mantle. Annual
295 Review of Earth and Planetary Sciences, 36, 389-420.

296 Grocke, S.B., Cottrell, E., de Silva, S., and Kelley, K.A. (2016) The role of crustal and
297 eruptive processes versus source variations in controlling the oxidation state of iron in
298 Central Andean magmas. Earth and Planetary Science Letters, 440, 92-104.

299 Hill, E., Blundy, J.D., and Wood, B.J. (2010) Clinopyroxene–melt trace element
300 partitioning and the development of a predictive model for HFSE and Sc.
301 Contributions to Mineralogy and Petrology, 161, 423-438.

302 Kelley, K.A., and Cottrell, E. (2009) Water and the oxidation state of subduction zone
303 magmas. Science 325, 605-607.

304 Kelley, K.A., and Cottrell, E. (2012) The influence of magmatic differentiation on the
305 oxidation state of Fe in a basaltic arc magma. Earth and Planetary Science Letters,
306 329-330, 109-121.

307 Lee, C.T., Leeman, W.P., Canil, D., and Li, Z. (2005) Similar V/Sc Systematics in
308 MORB and Arc Basalts: Implications for the Oxygen Fugacities of their Mantle
309 Source Regions. Journal of Petrology, 46, 2313-2336.

310 Lee, C.T., Luffi, P., Le Roux, V., Dasgupta, R., Albarede, F., and Leeman, W.P. (2010)
311 The redox state of arc mantle using Zn/Fe systematics. Nature 468, 681-685.

312 Lee, C.-T.A., Brandon, A.D., and Norman, M. (2003) Vanadium in peridotites as a proxy
313 for paleo-fO2 during partial melting. Geochimica et Cosmochimica Acta, 67, 3045-
314 3064.

315 Li, Z.-X., and Lee, C.-T. (2004) The constancy of upper mantle fO2 through time
316 inferred from V/Sc ratios in basalts. Earth and Planetary Science Letters, 228, 483-
317 493.

318 Li, Y., and Audétat, A. (2015) Effects of temperature, silicate melt composition, and
319 oxygen fugacity on the partitioning of V, Mn, Co, Ni, Cu, Zn, As, Mo, Ag, Sn, Sb, W,
320 Au, Pb, and Bi between sulfide phases and silicate melt. Geochimica et
321 Cosmochimica Acta, 162, 25-45.

322 Li, Y., and Audétat, A., 2012. Partitioning of V, Mn, Co, Ni, Cu, Zn, As, Mo, Ag, Sn, Sb,
323 W, Au, Pb, and Bi between sulfide phases and hydrous basanite melt at upper mantle
324 conditions. Earth and Planetary Science Letters, 355, 327-340.

Lundstrom, C.C., Shaw, H.F., Ryerson, F.J., Williams, Q., and Gill, J. (1998) Crystal chemical control of clinopyroxene-melt partitioning in the Di-Ab-An system: implications for elemental fractionations in the depleted mantle. Geochimica et Cosmochimica Acta, 62, 2849-2862.

Mallmann, G., and O'Neill, H.S.C. (2009) The Crystal/Melt Partitioning of V during Mantle Melting as a Function of Oxygen Fugacity Compared with some other Elements (Al, P, Ca, Sc, Ti, Cr, Fe, Ga, Y, Zr and Nb). Journal of Petrology, 50, 1765-1794.

Médard, E., McCammon, C.A., Barr, J.A., and Grove, T.L. (2008) Oxygen fugacity, temperature reproducibility, and H_2O contents of nominally anhydrous piston-cylinder experiments using graphite capsules. American Mineralogist, 93, 1838-1844.

Michely, L.T., Leitzke, F.P., Speelmanns, I.M., and Fonseca, R.O.C. (2017) Competing effects of crystal chemistry and silicate melt composition on trace element behavior in magmatic systems: insights from crystal/silicate melt partitioning of the REE, HFSE, Sn, In, Ga, Ba, Pt and Rh. Contributions to Mineralogy and Petrology, 172.

Pilet, S., Baker, M.B., and Stolper, E.M. (2008) Metasomatized lithosphere and the origin of alkaline lavas. Science 320, 916-919.

Righter, K., Sutton, S. R., Newville, M., Le, L., Schwandt, C. S., Uchida, H., Lavina, B., and Downs, R. T. (2006) An experimental study of the oxidation state of vanadium in spinel and basaltic melt with implications for the origin of planetary basalt. American Mineralogist, 91, 1643-1656.

346 Sutton, S. R., Karner, J., Papike, J., Delaney, J. S., Shearer, C., Newville, M., Eng, P.,
347 Rivers, M., and Dyar, M. D. (2005) Vanadium K edge XANES of synthetic and
348 natural basaltic glasses and application to microscale oxygen barometry. Geochimica
349 et Cosmochimica Acta, 69, 2333-2348.

350 Walter, M.J. (1998) Melting of garnet peridotite and the origin of
351 komatiite and depleted lithosphere. Journal of Petrology, 39, 29–60.

352 Wood, B.J., and Blundy, J.D. (2002) The effect of H_2O on crystal-melt partitioning of
353 trace elements. Geochimica et Cosmochimica Acta, 66, 3647-3656.

354

This is a preprint, the final version is subject to change, of the American Mineralogist (MSA)
Cite as Authors (Year) Title. American Mineralogist, in press.
DOI: https://doi.org/10.2138/am-2018-6464

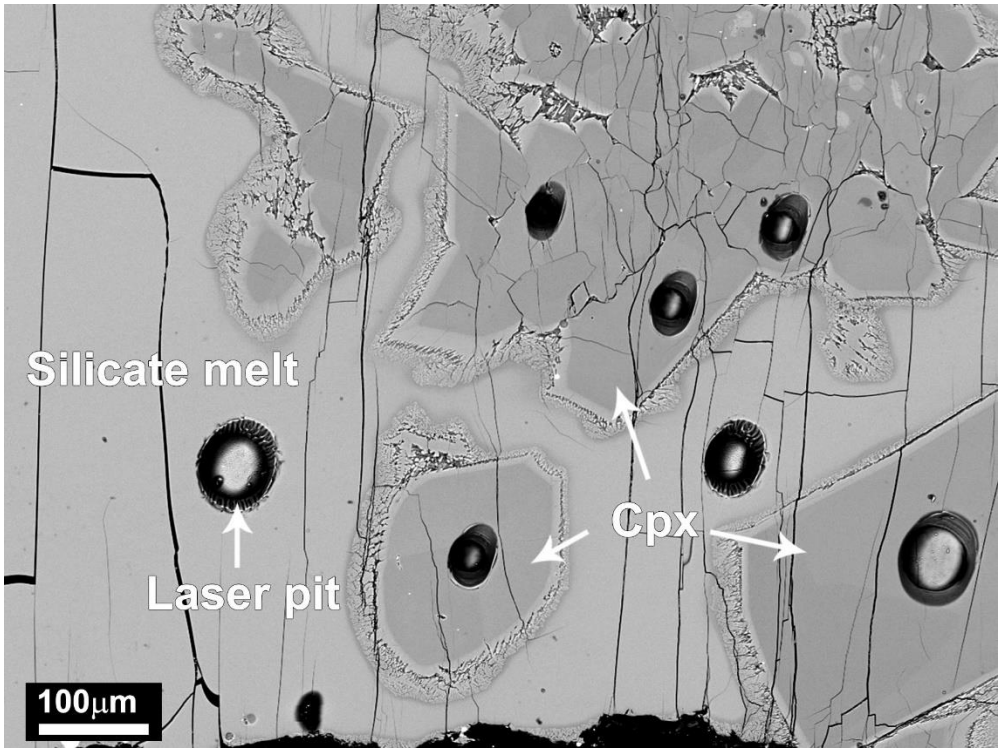

FIGURE 1. Backscattered electron image of typical run products, showing coexisting silicate melt and clinopyroxene (Cpx) synthesized at 1300 °C and 1.4 GPa (run W-5). Note that the dendritic material in the boundary between the clinopyroxene crystal and silicate melt was fine crystals produced from silicate melt during quench.

This is a preprint, the final version is subject to change, of the American Mineralogist (MSA)
Cite as Authors (Year) Title. American Mineralogist, in press.
DOI: https://doi.org/10.2138/am-2018-6464

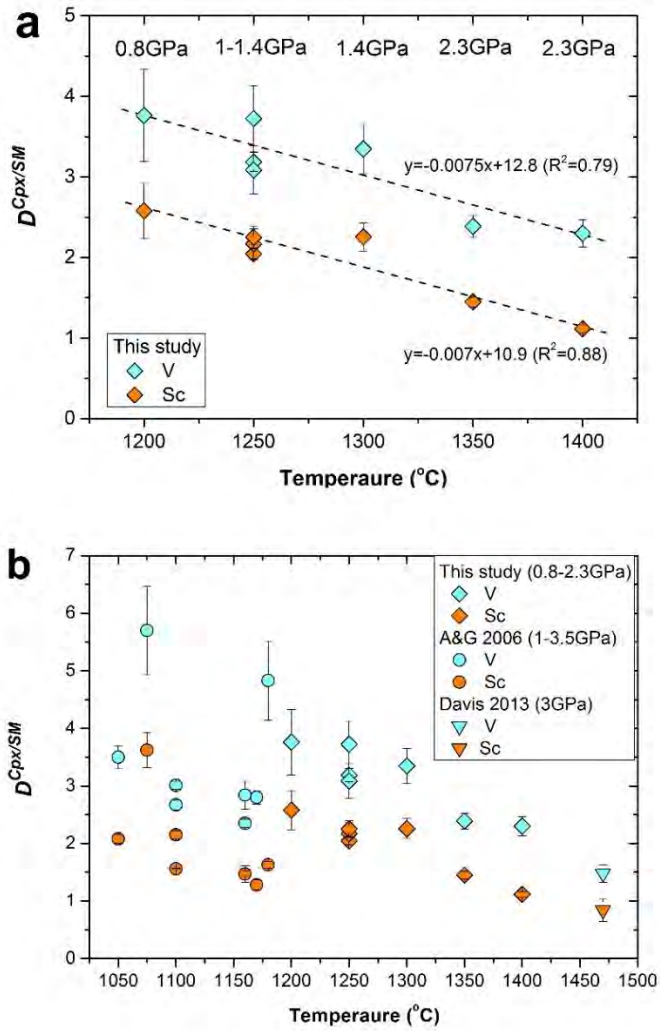

362

363 **FIGURE 2.** The variation of $D_V^{Cpx/SM}$ and $D_{Sc}^{Cpx/SM}$ as a function of experimental
364 temperature and pressure. Note that the regression of $D_V^{Cpx/SM}$ and $D_{Sc}^{Cpx/SM}$ data in panel
365 (a) yields similar slopes for V and Sc, indicating similar partitioning behavior of V and
366 Sc. The relatively low $D_V^{Cpx/SM}$ and $D_{Sc}^{Cpx/SM}$ from Adam and Green (2006) in panel (b)
367 could be partly due to the high melt water contents (see text for details). Note that all the
368 $D^{Cpx/SM}$ values plotted were simultaneously determined in experiments performed in
369 graphite-lined Pt or $Pt_{95}Rh_{05}$ capsules (Adam and Green 2006; Davis et al. 2013). The
370 silicate melt in Adam and Green (2006) is basanitic melt with 6-16 wt.% water, whereas
371 in Davis et al. (2013) it is nominally dry basaltic melt which is in equilibrium with KLB-
372 1 peridotite at ~1460 °C and 3 GPa.

This is a preprint, the final version is subject to change, of the American Mineralogist (MSA)
Cite as Authors (Year) Title. American Mineralogist, in press.
DOI: https://doi.org/10.2138/am-2018-6464

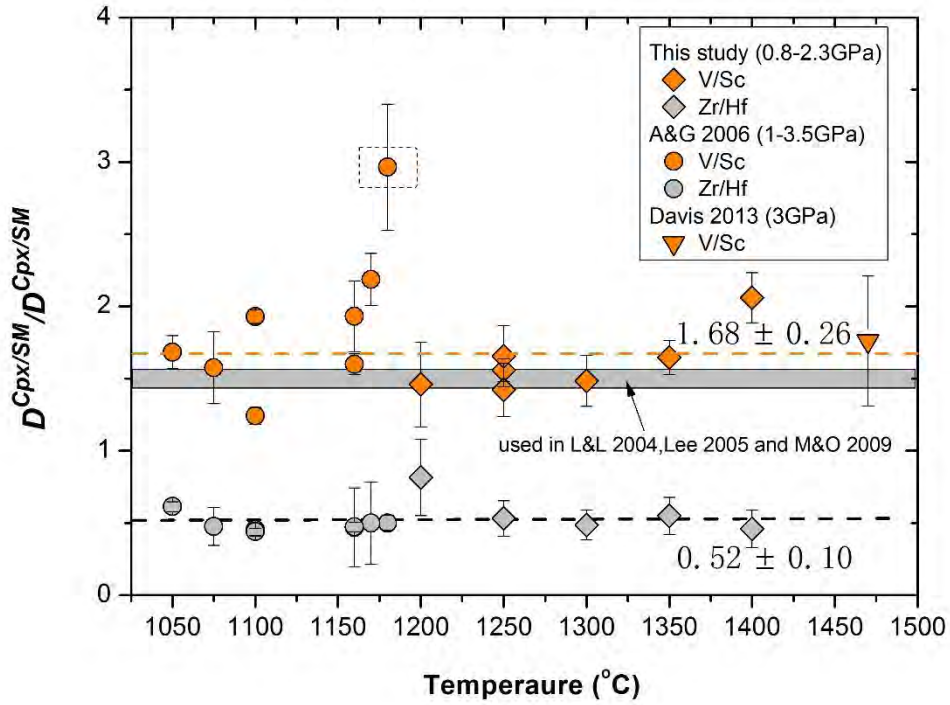

FIGURE 3. The variation of $D_V^{Cpx/SM}/D_{Sc}^{Cpx/SM}$ and $D_{Zr}^{Cpx/SM}/D_{Hf}^{Cpx/SM}$ as a function of experimental temperature and pressure. The $D_V^{Cpx/SM}/D_{Sc}^{Cpx/SM}$ and $D_{Zr}^{Cpx/SM}/D_{Hf}^{Cpx/SM}$ are nearly a constant of 1.68±0.26 (excluding the data point in the dash box) and 0.52±0.1, respectively, regardless of experimental temperature, pressure, melt composition, and melt water content, indicating that these factors cannot cause fractionation of V from Sc in mantle melts, as in the case for Zr and Hf, through clinopyroxene/silicate melt partitioning. Note that the $D_V^{Cpx/SM}/D_{Sc}^{Cpx/SM}$ of ~1.5 used in Li and Lee (2004), Lee et al. (2005), and Mallmann and O'Neill (2009) for fO_2 at ~FMQ-2 is very close to the $D_V^{Cpx/SM}/D_{Sc}^{Cpx/SM}$ obtained in this study, implying the valid use of $D_V^{Cpx/SM}$ and $D_{Sc}^{Cpx/SM}$ obtained at 1 bar and dry conditions to constrain mantle fO_2. For melt composition and water content, see Figure 2.

This is a preprint, the final version is subject to change, of the American Mineralogist (MSA)
Cite as Authors (Year) Title. American Mineralogist, in press.
DOI: https://doi.org/10.2138/am-2018-6464

TABLE 1. Summary of experimental conditions, major element (in wt.%) and trace element (in ppm) compositions of silicate melts and clinopyroxene, and the calculated partition coefficients of trace elements between clinopyroxene and silicate melt ($D^{Cpx/SM}$).

Run No	T (°C)	P (GPa)	$D_V^{Cpx/SM}$	$D_{Sc}^{Cpx/SM}$	$D_{Zr}^{Cpx/SM}$	$D_{Hf}^{Cpx/SM}$	Phase	SiO_2	TiO_2	Al_2O_3	FeO	Na_2O	K_2O	CaO	MgO	P_2O_5	Total	V	Sc	Zr	Hf
W-9	1200	0.8	3.8(0.6)	2.6(0.3)	0.58(0.17)	0.71(0.08)	melt	41.01(0.39)	4.48(0.05)	14.18(0.08)	8.74(0.12)	2.35(0.19)	1.21(0.11)	16.55(0.10)	8.42(0.28)	0.09(0.01)	96.76(0.74)	192(11)	39(2)	120(6)	4.1(0.3)
							Cpx	48.25(0.67)	2.34(0.31)	7.11(0.52)	4.27(0.49)	0.61(0.05)	<d.l	23.00(0.36)	13.83(0.64)	0.01(0.01)	99.59(0.66)	722(102)	99(12)	69(21)	2.9(0.2)
Y-1	1250	1	3.2(0.1)	2.0(0.1)	n.d	n.d	melt	42.18(0.36)	3.90(0.05)	11.99(0.11)	7.35(0.08)	1.71(0.05)	0.90(0.05)	17.26(0.20)	11.36(0.14)	0.07(0.01)	96.71(0.74)	318(6)	63(1)	n.d	n.d
							Cpx	49.66(1.10)	1.77(0.05)	6.44(0.09)	2.14(0.02)	0.29(0.01)	<d.l	23.70(0.50)	15.78(0.22)	0.01(0.00)	99.78(1.67)	1014(32)	129(4)	n.d	n.d
Y-4	1250	1	3.1(0.3)	2.2(0.2)	n.d	n.d	melt	42.52(0.39)	4.01(0.04)	12.33(0.14)	6.94(0.22)	1.72(0.10)	0.95(0.03)	17.18(0.17)	10.81(0.16)	0.07(0.01)	96.54(0.37)	327(2)	57(1)	n.d	n.d
							Cpx	51.48(0.80)	1.26(0.16)	4.77(0.28)	2.14(0.09)	0.21(0.02)	<d.l	24.24(0.32)	16.98(0.51)	0.01(0.00)	100.31(0.41)	1007(97)	124(11)	n.d	n.d
Y-3	1250	1.4	3.7(0.4)	2.3(0.1)	0.32(0.05)	0.60(0.10)	melt	40.75(0.38)	4.35(0.14)	13.36(0.26)	7.94(0.17)	1.30(0.24)	1.07(0.14)	16.26(0.55)	10.9(0.67)	0.09(0.01)	96.01(0.96)	227(23)	49(2)	138(2)	3.5(0.3)
							Cpx	49.96(0.96)	1.59(0.25)	6.96(0.32)	2.39(0.13)	0.32(0.03)	<d.l	23.68(0.22)	15.92(0.52)	0.01(0.00)	100.23(0.23)	845(37)	110(4)	44(7)	2.1(0.3)
W-5	1300	1.4	3.3(0.3)	2.3(0.2)	0.22(0.03)	0.44(0.07)	melt	41.94(0.43)	4.50(0.12)	13.92(0.20)	5.16(0.11)	2.08(0.08)	1.18(0.03)	15.99(0.29)	11.47(0.11)	0.08(0.01)	96.32(1.11)	259(9)	50(1)	147(3)	4.0(0.2)
							Cpx	49.41(1.33)	1.86(0.26)	7.55(0.84)	2.38(0.29)	0.34(0.07)	<d.l	23.24(0.45)	16.31(0.72)	0.01(0.00)	100.32(0.55)	865(73)	112(8)	32(5)	1.8(0.3)
W-7	1350	2.3	2.4(0.1)	1.5(0.1)	0.13(0.02)	0.23(0.04)	melt	39.66(0.31)	4.51(0.04)	12.66(0.15)	8.24(0.03)	1.91(0.03)	1.11(0.04)	15.2(0.13)	11.34(0.12)	0.08(0.01)	94.71(0.32)	295(4)	57(1)	147(2)	4.0(0.1)
							Cpx	49.74(0.33)	1.30(0.14)	8.53(0.27)	2.69(0.03)	0.60(0.05)	<d.l	22.69(0.41)	14.96(0.33)	0.02(0.01)	100.53(0.41)	704(40)	83(3)	18(3)	0.9(0.2)
W-11	1400	2.3	2.3(0.2)	1.1(0)	0.08(0.01)	0.18(0.04)	melt	41.89(0.47)	3.98(0.11)	11.9(0.17)	7.97(0.16)	1.54(0.19)	0.91(0.12)	16.66(0.52)	11.87(0.26)	0.07(0.01)	96.79(1.13)	323(11)	66(2)	125(1)	4.5(0.2)
							Cpx	50.65(0.44)	1.04(0.23)	7.49(0.87)	2.39(0.13)	0.54(0.04)	<d.l	22.69(0.55)	15.35(0.66)	0.01(0.00)	100.18(0.93)	743(48)	74(2)	10(2)	0.8(0.2)

Notes: For each sample,typically 10-20 spots and 5-15 spots were analyzed on each silicate phase using electron microprobe and LA-ICP-MS, respectively; all the experiments were run for 24 hours, except that run Y-4 was run for 48 hours; Cpx=clinopyroxene; SM=silicate melt. n.d=not determined; <d.l=below detection limit.